

## INFLUENCE OF MECHANICAL STRAINS ON ELECTROMAGNETIC SIGNALS OF A MICROSTRIP ANTENNA. FEM/BIM MODEL

N. ADNET<sup>\*</sup>, F. PABLO<sup>\*</sup>, I. BRUANT<sup>\*</sup> AND L. PROSLIER<sup>\*</sup>

<sup>\*</sup> Laboratoire Energétique Mécanique Electromagnétisme EA 4416 (LEME)  
Université Paris Ouest Nanterre La Défense  
50 rue de Sèvres, 92410 Ville d'Avray (France)  
e-mail: {nicolas.adnet, frederic.pablo, isabelle.bruant, laurent.proslier}@u-paris10.fr  
web page: <http://leme.u-paris10.fr>

**Key words:** mechanical/electromagnetic coupling, conformal cavity patch antenna, radar cross section, vector finite element, nodal finite element, boundary integral method, finite element method, Maxwell's equations.

**Abstract.** A hybrid numerical technique is proposed for a characterization of the radar cross section of a microstrip patch antenna residing in a dielectric filled cavity which is loaded by a sinusoidal mechanical pressure. A new 3D hexahedral finite element is developed in order to take into account the deformed shape of the antenna within the electromagnetic computations. The numerical tool combines the finite element and boundary integral methods to formulate a system for the solution of the fields at the aperture and those inside the cavity. In this work, numerical examples are presented for demonstrating the ability and the validity of the hexahedral element.

### 1 INTRODUCTION

The framework of the present study is the development of metamaterial strip antennas for aeronautical applications. This work is part of the MSIE project (Intelligent Materials and Structures for Electromagnetism), launched in 2008 by the competitiveness French cluster AStech. The aim of this project is the reduction of antennas on aircrafts using conformable microstrips made of metamaterials.

Such antennas, which are thin and conformable to planar or warped surfaces, can easily be embedded on any aircraft surfaces. Since these surfaces are subjected to aerodynamic and thermal loads, the influences of geometry change and mechanical strains on the electromagnetic signals of the antenna have to be studied. Available commercial predictive analysis tools appear not to be well suited for structural systems involving multiphysical couplings, and in particular electromagnetism.

The main difficulty in the solution of a problem involving deformable antennas is the accurate evaluation of the integrals over the unbounded domain of the electromagnetic radiation. Classical numerical methods for structural mechanics, such as Finite Element Method (FEM), require the discretisation of the domain far from the source region, which

leads to an excessive computational effort. An efficient solution consists in the combined Finite Element-Boundary Integral (FE-BI) Method [1], first developed in mechanical engineering and later introduced in electromagnetism.

This method consists in introducing a fictitious boundary that encloses the structures to be studied. Classical FEM is then used to approximate the fields in the interior domain, whereas the fields in the exterior region are evaluated by the boundary integral method. These fields are coupled at the fictitious boundary via the field continuity conditions. This leads to a coupled system of the interior and boundary fields to be solved.

The new numerical tool here proposed is based on a weak coupling between electromagnetism and mechanical behaviour. The FEM/BIM approach is used with a new dedicated 3D hexahedral finite element. The mechanical field is approximated through a classical nodal formulation while the electromagnetic one is expressed by an edge formulation [2]. This completely new software has been implemented from scratch and it has been validated through various benchmarks found in the literature [4]. This contribution presents an extension of the FEM/BIM technique applied to numerical simulations for the characterization of a patch antenna subjected to bending loads.

## 2 FORMULATION OF THE COUPLED PROBLEM

### 2.1 Geometric description

In the present work, the considered antennal structure is illustrated in **Figure 1**. It consists in a rectangular patch antenna residing on a cavity [1] recessed in an infinite ground plane. The cavity is filled with a homogeneous dielectric material having a relative permittivity  $\epsilon_r$  and a relative permeability  $\mu_r$ . The antenna thickness is assumed to be smaller than the substrate height. Therefore, it will be neglected in the following developments. Furthermore, this structure is supposed to be integrated on composite aircraft panels.

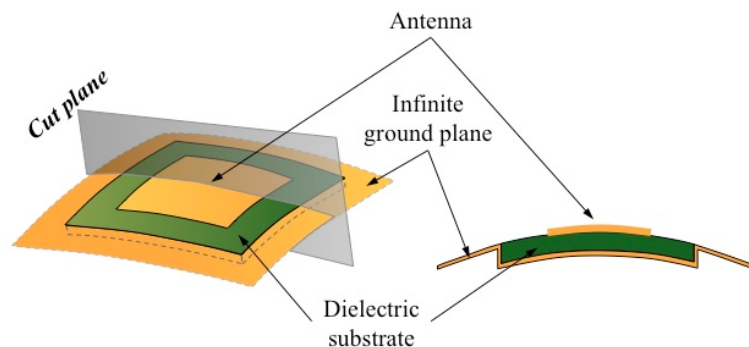


**Figure 1:** Studied one patch antenna

In the following sections, the free space region above the cavity and the ground plane, and below these ones will be respectively denoted by  $V_\infty$  and  $V$  symbols (see **Figure 2**).

The antenna is studied in a receiving run mode. Thus, the cavity is illuminated by electromagnetic waves emitted by a source point of the region  $V_\infty$ . Considering the Cartesian coordinate system presented in the **Figure 3**, the incident wave, emitted from a source point  $M'$

and received by an observation point  $M$ , is respectively located by the following position vectors  $\vec{r}' = \overline{OM'}$  and  $\vec{r} = \overline{OM}$ . The related Euclidian norms are defined by  $r' = \|\vec{r}'\| = \sqrt{x'^2 + y'^2 + z'^2}$  and  $r = \|\vec{r}\| = \sqrt{x^2 + y^2 + z^2}$ .

At last, the cavity is assumed to be subjected to some mechanical loads such as pressures. The governing equations and variational formulations are presented in the next sections.

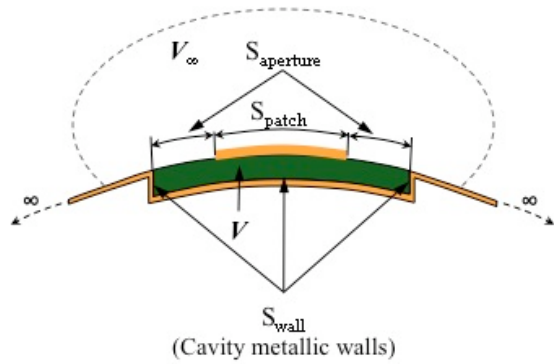


Figure 2: The cavity model and its surrounding regions

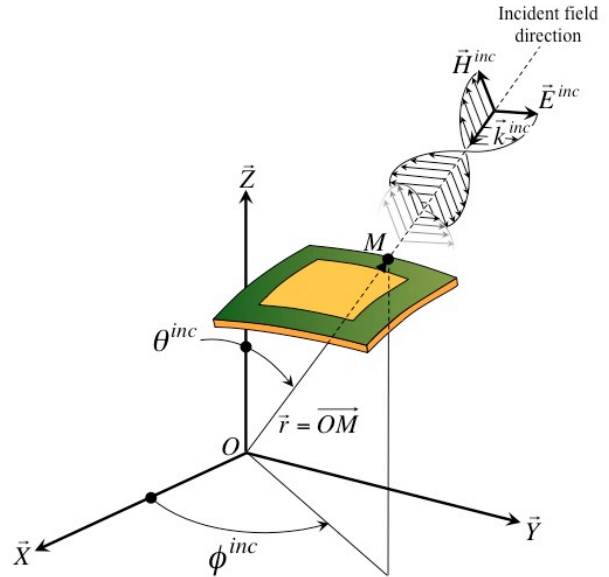


Figure 3: The incident field and the Cartesian coordinate system

## 2.2 Mechanical governing equations and weak form

Assuming the antenna is embedded on a composite panel, the cavity volume  $V$  will be subjected to mechanical distortions of its support. Taking into account strains in the electromagnetic computations is then essential.

Considering a static approach, the mechanical governing equations consists in the equilibrium equation, the constitutive equation in  $V$  and the strain-displacement relationship [3] :

$$\overline{\text{div}}T + \vec{f} = \vec{0} \quad (1)$$

$$T = CS(\vec{u}) \quad (2)$$

$$S(\vec{u}) = \frac{1}{2}(\text{grad}\vec{u} + \text{grad}^T\vec{u}) \quad (3)$$

where  $T$ ,  $S(\vec{u})$ ,  $\vec{f}$  and  $C$  are respectively the stress tensor, the strain tensor, the prescribed body forces vector applied to  $V$  and the elastic stiffness tensor. In addition to these equations, one has to take into account the mechanical boundary conditions : a first one where mechanical vector displacement  $\vec{u}$  is imposed, and the second one where a surface force vector  $\vec{F}$  is applied on the boundary  $\partial V_F$ .

The weak form of the mechanical boundary value problem is then given by :

find  $\bar{u} \in U_{ad}$  such that : (4)

$$\int_V S^*(\bar{u}^*) : T(\bar{u}) dV = \int_V \bar{u}^* \vec{f} dV + \int_{\partial V_f} \bar{u}^* \vec{F} dS$$

for any admissible virtual displacement  $\bar{u}^* \in U_{ad}^*$ . This variational principle is the usual starting point for any finite element approximation in mechanical modelling.

### 2.3 Electromagnetic governing equations and weak form

Here, the FEM/BIM technique [4] is used. The proposed method involves the equivalence principle to subdivide the original problem into two equivalent problems. They are then coupled by enforcing field continuity. The fields in each region are subsequently formulated via a variational or integral equation approach leading to a coupled set of integral equations solved via the finite element method.

#### 2.3.1 The governing equations

The Maxwell's equations (in the usual time harmonic convention  $e^{j\omega t}$ ) and the constitutive relations are :

$$\overrightarrow{rot} \vec{E} = -j\omega \mu_r \mu_0 \vec{H} \quad (5)$$

$$\overrightarrow{rot} \vec{H} = j\omega \varepsilon_r \varepsilon_0 \vec{E} \quad (6)$$

$$div(\vec{D}) = \rho \quad (7)$$

$$div(\vec{B}) = 0 \quad (8)$$

$$\vec{D} = \varepsilon_0 \varepsilon_r \vec{E}, \quad \vec{B} = \mu_0 \mu_r \vec{H} \quad (9)$$

where  $\vec{D}$ ,  $\vec{B}$ ,  $\varepsilon_0$ ,  $\mu_0$  and  $\rho$  respectively are the electric flux density related to the  $\vec{E}$  field, the magnetic flux density related to the  $\vec{H}$  field, the permittivity and the permeability in the free space region and the electric charge density.

#### 2.3.2 Boundary conditions and loads

- *The excitation vector* : Considering the antenna runs in a receiving mode, the excitation vector is defined by the incident plane wave model [4]. The propagation direction of the travelling wave is defined by  $\vec{k}^{inc}$ . Thus, the excitation vector received by an observation point located by  $\vec{r}$  is given as a function of the electric field polarisation  $\vec{E}_0$  and the wavenumber  $k_0$  by :

$$\vec{E}^{inc} = \vec{E}_0 e^{-j k_0 \vec{k}^{inc} \cdot \vec{r}} \quad (10)$$

- *The perfect electric conductor* : the boundary conditions associated to the cavity model are those of perfect electric conductors prescribed on the cavity walls indicated in the **Figure 2**. They enforce no tangential electric fields on the metallic regions such as the

patch and the ground plane :

$$\vec{n} \wedge \vec{E} = \vec{0} \quad (11)$$

- *The integral equation on the aperture surface  $S$*  : in accordance with the equivalence principle [4], the fields existing in the free space region (above the ground plane) are then due to the radiation caused by the equivalent magnetic currents  $\vec{M} = \vec{E} \wedge \vec{n}$  residing on the ground plane. Accordingly, the magnetic field  $\vec{H}^{ext}$  created by  $\vec{M}$  in the external region is defined by :

$$\vec{H}^{ext} = 2\vec{H}^{inc} - 2j\frac{k}{Z_0} \iint_S \overline{\overline{G_0}}(\vec{r}, \vec{r}') (\vec{E} \wedge \vec{n}) dS' \quad (12)$$

where  $\vec{H}^{inc}$  denotes the magnetic field due to an incident wave,  $Z_0$  is the intrinsic impedance in free space and  $\overline{\overline{G_0}}$  is the free space dyadic Green's function [5]. Enforcing continuity of the tangential electric fields across the interface  $S$ , the fields in both the internal and external regions are then coupled :

$$\vec{n} \wedge \begin{cases} \vec{E}^{int} \\ \vec{H}^{int} \end{cases} = \vec{n} \wedge \begin{cases} \vec{E}^{ext} \\ \vec{H}^{ext} \end{cases} \quad (13)$$

where the superscripts *int* and *ext* respectively denote the fields created in the internal region  $V$  and the unbounded external region  $V_\infty$ .

### 2.3.3 Weak form formulation

Considering the equations (5) to (13), the variational principle leads to the weak form of the electromagnetic problem :

$$\text{find } \vec{E} \in E_{ad} \text{ such that :} \quad (14)$$

$$b(\vec{E}, \vec{E}^*) = c(\vec{E}^*)$$

for all admissible virtual electric field  $\vec{E}^* \in E_{ad}^*$ , with :

$$\begin{aligned} b(\vec{E}, \vec{E}^*) = & \int_V \overrightarrow{rot} \vec{E}^* \mu_r^{-1} \overrightarrow{rot} \vec{E} dV - k_0^2 \int_V \vec{E}^* \epsilon_r \vec{E} dV \\ & + k_0^2 \int_S \int_S \vec{E}_S^* (\vec{n} \wedge \overline{\overline{G_0}}(\vec{r}, \vec{r}') \wedge \vec{n}') \vec{E}'_S dS' dS \end{aligned} \quad (15)$$

$$c(\vec{E}^*) = -2jk_0 \int_S (\vec{n} \wedge \vec{E}_S^*) (\vec{k}^{inc} \wedge \vec{E}^{inc}) dS \quad (16)$$

where  $S = S_{aperture}$  represents the aperture zone of the cavity that is not covered by the metallic patch as illustrated in **Figure 2**. The  $\vec{n}$  and  $\vec{n}'$  denote the normals associated to the observation point  $M$  and the source point  $M'$  lying on the aperture area. The fields  $\vec{E}$  and  $\vec{E}_S$  are respectively the internal and aperture electric fields.

A difficulty in the evaluation of this quadruple surface integral within (15) is the usual singularity associated with the derivatives of the free space Green's function. This can be

numerically computed by considering two different Gauss quadratures, each is related to the observation surface ( $S$ ) and the source surface ( $S'$ ).

### 3 SOLVING THE COUPLED PROBLEM

#### 3.1 Weak form of the coupling

The mechanical behaviour of the antenna is assumed to be non sensitive to the electromagnetic phenomena. Therefore, a weak coupling between the electromagnetic part and the mechanical one is considered. The problem can be studied in two successive steps :

- firstly, the mechanical problem (4) is solved in order to compute the deformed shape of the antenna. The displacements are interpolated at the element nodes.
- secondly, the computation of the electromagnetic problem (14) is done by taking into account the deformed mesh.

#### 3.2 A 3D hexahedral vector/node-based element

The antenna is meshed using 3D hexahedral finite elements (see **Figure 4**). The same element is used to solve either the mechanical or the electromagnetic problem. In order to ensure the compatibility between the two physical domains, the mechanical displacements are linearly interpolated at the 8 nodes of the element :

$$\vec{u} = \sum_{n=1}^8 N_n(\xi, \eta, \zeta) \vec{u}_n \quad (17)$$

whereas the electric fields are approximated through the 12 edges of those :

$$\vec{E} = \sum_{n=1}^{12} \vec{W}_n(\xi, \eta, \zeta) E_n \quad (18)$$

The  $N_n$  are the classical nodal shape functions of a hexahedra while  $\vec{W}_n$  are the vector shape functions [1] related to this kind of finite element. In (19), the quantities  $E_n$  represents the electric field magnitude lying on the hexahedra edges.

Through this way, the hexahedral elements are able to take into account the deformed shape information when performing the electromagnetic computation. By virtue of the finite element method, the technique is then pertinent to study a patch antenna residing on a dielectric substrate that is mechanically loaded.

Introducing the field approximations in equations (4) and (14), the mechanical discretized problem can be written as the following form :

$$K_{FEM} \{q_U\} = \{F_{ext}\}_{mech} \quad (19)$$

where  $K_{FEM}$ ,  $\{q_U\}$  and  $\{F_{ext}\}_{mech}$ , are respectively the stiffness matrix, the unknown displacements and the mechanical excitation vector. For the electromagnetic problem, one obtains :

$$\left(Y_{FEM} - k_0^2(L_{FEM} - L_{BIM})\right)\{q_E\} = \{F_{ext}\}_{em} \quad (20)$$

where  $Y_{FEM}$ ,  $L_{FEM}$ ,  $L_{BIM}$ ,  $\{q_E\}$  and  $\{F_{ext}\}_{em}$  represent respectively the admittance matrix, the inductance matrices related to the interior and the exterior fields, the unknown electric fields and the electromagnetic excitation vector. The subscripts  $FEM$  and  $BIM$  denote the matrices that are resulting from the discretization of the interior volume  $V$  and the aperture region  $S$ .

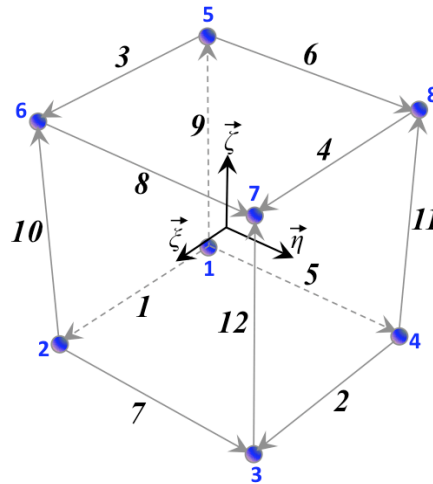


Figure 4: The 3D hexahedral vector/node-based finite element

#### 4 NUMERICAL VALIDATION

In order to validate the coupling formulation, a numerical test presented in [4] is considered. It consists in computing the radar cross section (RCS) of a patch antenna as a function of its curvature. In the test, the deformed shape of the antenna is just controlled by the curvature radius. In this section, the RCS of the same antenna is computed with a deformed mesh resulting from a mechanical pressure load.

The radar cross section  $\sigma$  is computed from the scattered magnetic fields  $\vec{H}^{far}$  and is defined by :

$$\sigma = \lim_{r \rightarrow \infty} 4\pi r^2 \frac{|\vec{H}^{far}|^2}{|\vec{H}^{inc}|^2} \quad (21)$$

where  $|\vec{H}^{inc}|^2$  is equal to unity. The RCS is usually normalized to  $\lambda^2$ , the squared wavelength.

The scattered magnetic fields result from the integration of the surface magnetic currents emitted by a test point  $M'$  lying on the aperture surface  $S$ , and received by an observation point  $M$  located at the infinity space :

$$\vec{H}^{far} = j \frac{k_0}{Z_0} \int_S \vec{G}_0(r, r') (\vec{n} \wedge \vec{E}'_S) dS' \quad (22)$$

### 4.1 Geometric description of the benchmark

The structure consists in a rectangular patch residing in a dielectric filled cavity, which the relative permittivity is  $\epsilon_r = 2.17$ , the relative permeability is  $\mu_r = 1.00$  and the Young modulus is about  $E = 1\,000$  MPa. The patch dimensions are 20 mm x 30 mm and the cavity size is 50 mm x 60 mm x 0.7874 mm. The antenna is simply supported along the  $y$  direction at  $x = 0$  and is mechanically loaded by a sinusoidal pressure :

$$p = p_0 \sin\left(\pi \frac{x}{L}\right) \tag{23}$$

where  $L = 50$  mm here.

Considering a receiving antenna, the electromagnetic excitation is a vertical incident field and set for a transversal magnetic polarisation ( $\alpha = 0^\circ$ , see Figure 5).

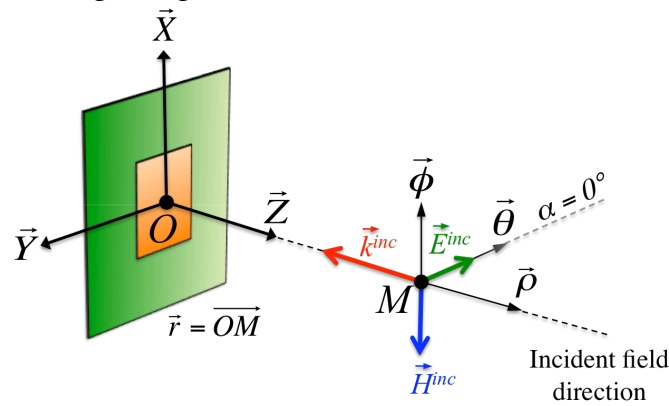
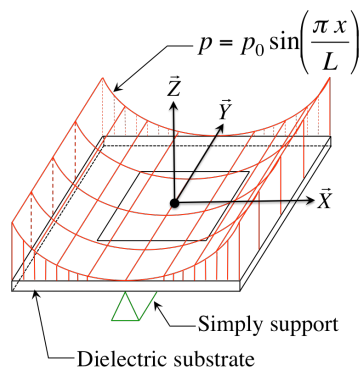


Figure 5: Incident field and polarisation setup

The sensitivity of the RCS to the curvature is studied with respect to various pressure magnitudes  $p_0$  and with respect to a frequency range going from 4.0 GHz to 6.0 GHz. The magnitudes  $p_0$  listed in Table 1 were chosen in order to match two curvatures studied by [4] for the considered antenna. Figure 6 presents two configurations of the strained antenna resulting from the cylindrical pressure  $p$ .



Pressure magnitude $p_0$	Associated curvature radius $R$
$0.54 \times 10^{-3}$ MPa	2 000 mm
$7.21 \times 10^{-3}$ MPa	150 mm

Table 1: Curvature radii as a function of the mechanical pressure  $p$  loading the antenna



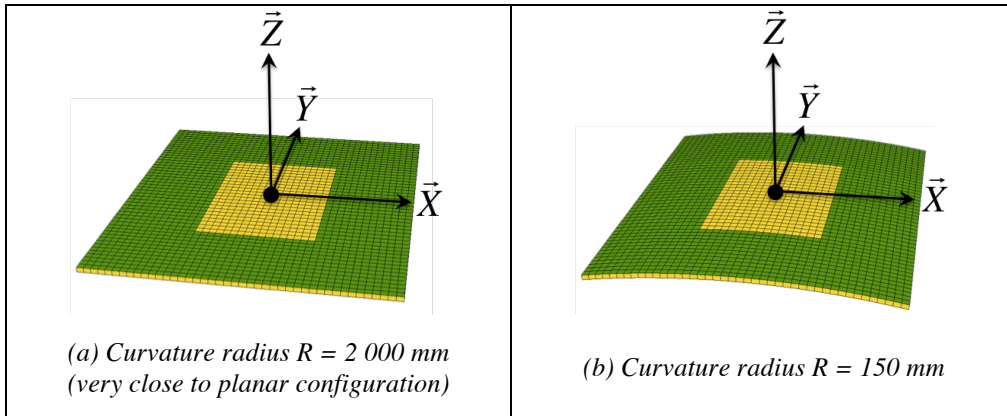


**Figure 6:** Configurations of the strained patch antenna loaded by a sinusoidal pressure

#### 4.2 RCS as a function of the frequency

The backscattered RCS of the antenna are shown in **Figure 7**. They are related to the planar and the curved cases which the curvature radii  $R = 150$  mm and  $R = 2\,000$  mm. The results performed with the hexahedral elements are in good agreement with the brick elements simulations done in [4]. The resonance frequencies and the dB levels are similar with both the hexahedra and brick finite elements. As expected for a very large radius (2 000 mm), it can be seen that the planar and the curved RCS are nearly merged. A 19% RCS shift is noticed for the 150 mm curved configuration. Therefore, the planar configuration represents an envelope for infinite radii of curvature and bounds lower ones.

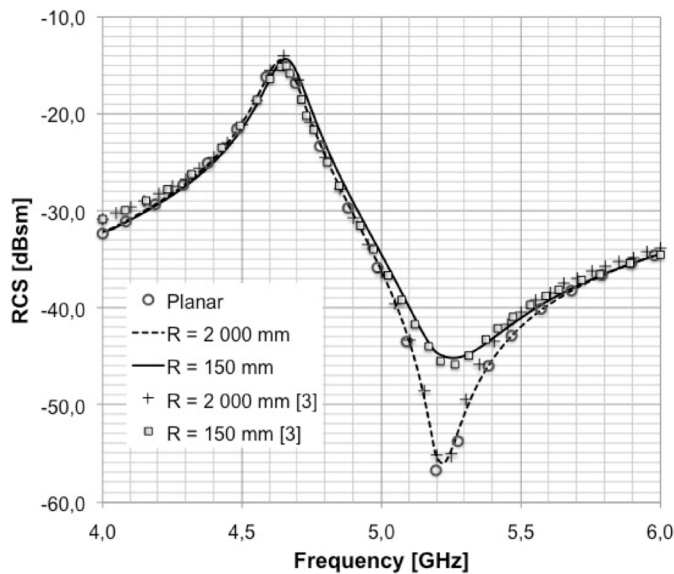


**Figure 7:** RCS of a patch antenna related to a planar and two cylindrical structural configurations

Conversely, an important point has to be underlined concerning the numerical treatment of the BIM part. Our solutions are computed with two different Gauss quadratures whereas an

exact form of the planar Green's function contribution is considered in the computational process used in [4]. Moreover, the ability of hexahedral elements to take into account each node coordinates allows both planar and conformal configurations to be computed through the same element. For brick elements, treating planar and conformal shape needs to implement a *planar* and a *curved* brick element respectively. In the future, the hexahedral elements will enable us to treat more arbitrary strained structures than using bricks and furthermore, to investigate the effects of singly or doubly curvatures on the RCS.

## 5 CONCLUSIONS

The presented work concerns the computation of the RCS property of a patch antenna loaded by a sinusoidal mechanical pressure. A weak coupling between the electromagnetic and the mechanical domains was assumed. The simulations were performed through the FEM/BIM method considering a new 3D hexahedral finite element that combines the interpolation of the electromagnetic fields (at the element edges) and the mechanical fields (at the nodes of the hexahedra). Then, the main feature of the hexahedral element is the ability to take into account the deformed shape of the antenna within the electromagnetic computations.

Moreover, the FEM/BIM technique allows the computational domain to be only reduced to the structure volume since the unbounded external region is modelled through the BIM and then avoid the free space to be meshed.

The good agreement between the numerical results and the literature ones confirms the validity of the hexahedral element and the ability of the method to be applied to simulate the mechanic/electromagnetic coupled problem for a cylindrical conforming context. In order to enlarge the use of this work, more a kind of mechanical loads imposed on the antenna has to be considered such as twisting loads.

## REFERENCES

- [1] Jin, J.M. *The finite element method in Electromagnetics*. Wiley-Interscience. 2<sup>nd</sup> edition (2002).
- [2] Nédélec, J. C. *A new family of mixed elements in  $R^3$* . Numerical Mathematics, Vol. **50**, (1986) pp. 57-81.
- [3] Fung, Y.C. *Foundations of Solid Mechanics*. Prentice-Hall, Inc (1965).
- [4] Volakis, J.L. Chatterjee, A. and Kempel L.C. *Finite Element Method for Electromagnetics; Antennas, Microwave circuits and scattering applications*. IEEE Press (1998).
- [5] Jin, J.M. and Volakis, J.L. *A hybrid finite element method for scattering and radiation by microstrip patch antennas and arrays residing in a cavity*. IEEE Trans. Ant. Propagat., (1991) 39(11):1598-1604.
- [6] Idelsohn, S.R. and Oñate, E. Finite element and finite volumes. Two good friends. *Int. J. Num. Meth. Engng* (1994) **37**:3323-3341.